

Sub-millimeter in-plane spatial resolution CINE imaging of the heart at 7.0 T using a 16 channel bow tie antenna transceiver coil array

Celal Oezerdem¹, Lukas Winter¹, Andreas Graessl¹, Katharina Paul¹, Antje Els¹, and Thoralf Niendorf^{1,2}

¹Berlin Ultra-High Field Facility (B.U.F.F.), MDC, Berlin, Germany, ²Experimental and Clinical Research Center, a joint cooperation between Charité Medical Faculty and the Max Delbrueck Center, Berlin, Germany

Target audience: Basic researchers and clinical scientists interested in novel MR technology applications at ultrahigh fields (UHF) including 7.0 T.

Purpose: Early UHF-CMR applications demonstrated the feasibility of cardiac chamber quantification at 7.0 T [1-3]. These efforts hold the promise to gain a better insight into myocardial microstructure including the visualization of myocardial clefts or crypts related to myocardial fiber or fascicle disarray which demands further enhancements in spatial resolution. This is a powerful motivator for improving the sensitivity of RF coil technology tailored for cardiac MR at 7.0 T. In this light dipole antenna TX/RX configurations offer improvements in signal-to-noise-ratio (SNR) and B_1^+ efficiency versus conventional configurations [4, 5], which would be beneficial for high spatial resolution imaging of the heart. For all these reasons this work investigates the capabilities of a sixteen channel bow tie dipole transceiver cardiac array for sub-millimeter spatial resolution of the heart at 7.0 T. For this purpose numerical field simulations are performed to ensure that the array is in full compliance with RF power deposition safety guidelines. A phase setting is derived to afford uniform and efficient excitation of the whole heart. 2D CINE FLASH imaging of the heart is performed in healthy subjects using an in-plane spatial resolution as high as $(0.8 \times 0.8) \text{ mm}^2$.

Methods: The transceiver cardiac array consists of 16 independent building blocks (Figure 1). Each of the building blocks contains a bow tie shaped $\lambda/2$ -dipole antenna (Figure 1) immersed in deuteriumoxide (D_2O) as high dielectric medium. 8 bow tie antenna building blocks were combined to form the anterior coil section and 8 building blocks were used to constitute the posterior coil section (Figure 1). EMF and SAR_{10g} simulations were performed using CST Studio Suite 2011 (CST AG, Darmstadt, Germany) together with human voxel models Duke (BMI: 23.1 kg/m²) and Ella (BMI: 22 kg/m²) from the Virtual Family. For transmission field shaping a phase based shimming approach based on EMF simulations was applied [6]. To find a phase setting, which satisfies the criteria for uniform and efficient excitation in the region of the heart a merit function was implemented and solved using a nonlinear solver (MATLAB, MathWorks, Natick, USA) based on the Levenberg-Marquardt algorithm. The phase setting deduced from shimming algorithm was incorporated into the splitting network hardware connected to the 16 bow tie antenna array using phase shifting coaxial cables. Using a 7.0 T whole body MR system (Magnetom, Erlangen, Germany) 2D CINE FLASH images of a four chamber view and a mid-ventricular short axis view of the heart were acquired using a twofold acceleration with the following spatial resolutions (i) $(1.8 \times 1.8 \times 6.0) \text{ mm}^3$, matrix size = 208×172 , (ii) $(1.4 \times 1.4 \times 4.0) \text{ mm}^3$, matrix size = 256×208 , (iii) $(1.1 \times 1.1 \times 2.5) \text{ mm}^3$, matrix size = 260×320 and (iv) $(0.8 \times 0.8 \times 2.5) \text{ mm}^3$, matrix size = 380×464 . An MR stethoscope (EasyACT, MRI.TOOLS GmbH, Berlin, Germany) was used for retrospective gating resolving the cardiac cycle into 30 cardiac phases. For data assessment the signal intensity profiles along a circumferential trajectory inside the myocardium were plotted for a mid-ventricular short axis view at end-diastole for all spatial resolutions. The profile curves were assigned according to standardized myocardial segmentation for tomographic imaging of the heart [7].

Results: As surveyed in Figure 2 and 3 four chamber view and short axis view images of the heart obtained with a standardized CMR protocol with a spatial resolution of $(1.8 \times 1.8 \times 6.0) \text{ mm}^3$ (a) were compared with images of an enhanced spatial resolution of $(1.4 \times 1.4 \times 4.0) \text{ mm}^3$ (b), $(1.1 \times 1.1 \times 2.5) \text{ mm}^3$ (c) and $(0.8 \times 0.8 \times 2.5) \text{ mm}^3$ (d). The latter protocol reduced the voxel size from 19.4 mm^3 down to 1.6 mm^3 and afforded a twelve-fold improvement in spatial resolution versus a standardized clinical CMR protocol. The overall image quality and the high spatial resolution enabled the visualization of fine subtle anatomical structures including the compact layer of the lateral right ventricular wall and the remaining trabecular layer. Pericardium, mitral and tricuspid valves and their associated papillary muscles and trabeculae were identifiable. For the short axis views shown in Figure 3 the analysis of the signal intensity distribution revealed a standard deviation in percentage of the mean value of the myocardium of 19 % for a spatial resolution of $(1.8 \times 1.8 \times 6.0) \text{ mm}^3$, 20 % for a spatial resolution of $(1.4 \times 1.4 \times 4.0) \text{ mm}^3$, 19 % for a spatial resolution of $(1.1 \times 1.1 \times 2.5) \text{ mm}^3$ and 21 % for a spatial resolution of $(0.8 \times 0.8 \times 2.5) \text{ mm}^3$.

Discussion and Conclusion: This work showed that high resolution CINE imaging of the heart at 7.0 T is feasible. The proposed bow tie antenna array supports a spatial resolution of $(0.8 \times 0.8 \times 2.5) \text{ mm}^3$ for 2D CINE FLASH imaging of the heart, This fidelity approaches an effective anatomical spatial resolution – voxel size per anatomy – which resembles that demonstrated for animal models [8]. These improvements will be beneficial for the assessment of subtle anatomical features such as trabeculae, for imaging myocardial tissue microstructure using T_2^* mapping and quantitative susceptibility mapping, for the visualization of myocardial clefts or crypts related to myocardial fiber or fascicle disarray and for extending morphologic assessment to the right ventricle.

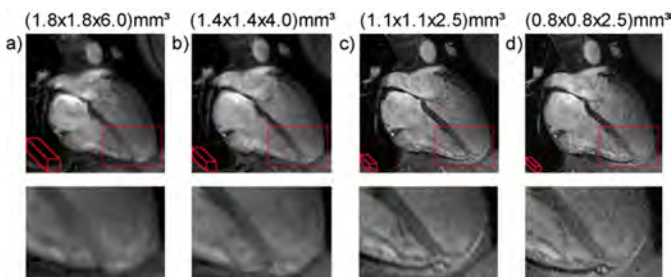


Figure 2: Top Four chamber view of the heart derived from 2D CINE FLASH with a spatial resolutions of **a)** standardized clinical protocol: $(1.8 \times 1.8 \times 6.0) \text{ mm}^3$, **b)** $(1.4 \times 1.4 \times 4.0) \text{ mm}^3$, **c)** $(1.1 \times 1.1 \times 2.5) \text{ mm}^3$, **d)** $(0.8 \times 0.8 \times 2.5) \text{ mm}^3$. **Bottom** Magnified views covering portions of the right ventricle and the ventricular trabeculae to outline the enhancements in the delineation of subtle anatomical details of the heart when using a factor of 12 improved spatial resolution vs the conventional protocol

References: [1] Brandts, et. Al. MRM 2010 [2] von Knobelsdorf-Brenkenhoff, et. Al., Eur. Radiol 2010 [3] Suttie, et. Al., NMR Biomed. 2012 [4] Raaijmaker, MRM 2011 [5] Ipek, Phys. Med. Biol. 2012 08 [6] Bitz, et. Al., MRM 2010 [7] Cerqueria, et. Al., Int J Cardiovasc Imaging 2002, [8] Wagenhaus, et. Al., PLoS One 2012

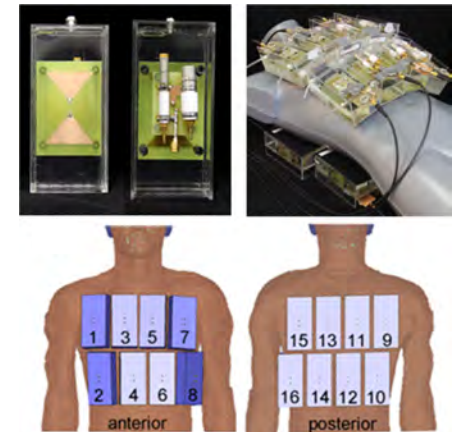


Figure 1: Photographs taken from the front and back of the bow tie antenna building block and the 16 channel cardiac array placed on a mannequin (**top row**). Elements of the cardiac array placed around the human voxel model Duke used for the numerical electromagnetic field simulations (**bottom row**).

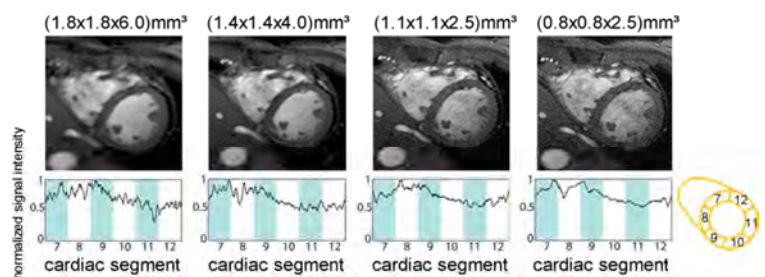


Figure 3: Top Short axis views of the heart derived from 2D CINE FLASH acquisitions using spatial resolution as good as $(0.8 \times 0.8 \times 2.5) \text{ mm}^3$. **Bottom row** Analysis of the signal intensity profile along a circular trajectory following the standardized segmentation of the myocardium.